scientific reports

Check for updates

OPEN

Interfacial coupling effect of Cr_2O_3 on the magnetic properties of $Fe_{72}Ga_{28}$ thin films

I. Hontecillas[1], M. Maicas[2], J. P. Andrés[3] & R. Ranchal[1,4]✉

Here it is investigated the effect of the antiferromagnet Cr_2O_3 on the magnetic properties of ferromagnetic $Fe_{72}Ga_{28}$ thin films. Sputtered $Fe_{72}Ga_{28}$ layers have their magnetization in the sample plane with a magnetic fluctuation that gives rise to magnetic ripple. In order to turn its magnetization into the out of plane (OOP) direction, it has been magnetically coupled with Cr_2O_3 that has magnetic moments along the *c*-axis, that is the perpendicular direction when properly aligned. Cr_2O_3 has been obtained from Cr oxidation, whereas $Fe_{72}Ga_{28}$ has been deposited on top of it by sputtering in the ballistic regime. Although a uniaxial in-plane magnetic anisotropy is expected for $Fe_{72}Ga_{28}$ thickness above 100 nm, the interfacial coupling with Cr_2O_3 prevents this anisotropy. The formation of stripe domains in $Fe_{72}Ga_{28}$ above a critical thickness reveals the enhancement of the out of plane component of the $Fe_{72}Ga_{28}$ magnetization with respect to uncoupled layers. Due to the interface coupling, the $Fe_{72}Ga_{28}$ magnetization turns into the out-of-plane direction as its thickness is gradually reduced, and a perpendicular magnetic anisotropy of $3{\cdot}10^6$ erg·cm^{-3} is inferred from experimental results. Eventually, the coupling between Cr_2O_3 and $Fe_{72}Ga_{28}$ promotes an exchange-bias effect that has been well fitted by means of the random field model.

Control of the magnetization is an important issue for the development of pioneering magnetic devices. Typically, thin films have the magnetization in the sample plane in order to reduce the energy of the system[1]. However, in many applications as for example: high density magnetic storage, spintronic devices, non-volatile random access memories, logic devices, skyrmions or sensors, materials with OOP magnetization are desirable[2–6].

Systems with large perpendicular magnetic anisotropy (PMA) such as $L1_0$ FePt and CoPt thin films are extensively investigated but, their large coercivity and switching fields can represent a drawback for their integration in devices[7,8]. Therefore, it is of interest the investigation of other materials with PMA, or the possibility of turning the magnetization into the OOP direction. Stripe domains appear above a critical thickness when a moderate PMA is present[9]. In permalloy films, stripes have been observed because of columnar growth[10], but they have also been promoted when coupled with NdCo[11]. Recently, the magnetization direction has been tuned in Fe–N layers by ion implantation and heat treatment conditions[9], and by annealing in $Fe_{87}Si_9B_{13}$[12]. Even more notably, the control of the magnetic anisotropy by means of voltage has been observed at magnetic transition metal/oxide interfaces[2].

FeGa alloys are extensively studied because of their large magnetostriction constant and low coercivity[13–16]. Also interesting is the possibility in sputtered $Fe_{72}Ga_{28}$ layers of controlling the in-plane magnetic anisotropy by growth conditions[17–19] or by thermal treatments combined with mechanical stress[20]. Molecular beam epitaxy (MBE) FeGa can exhibit domain stripes due to a low PMA[21–23], but the general behavior observed by magnetic force microscopy (MFM) in FeGa deposited either by electrodeposition[24], sputtering[25] or even MBE[26] is a magnetic ripple due to magnetic fluctuations in layers with magnetization in the sample plane.

In this work, we have explored the possibility of turning the $Fe_{72}Ga_{28}$ magnetization into the OOP direction when appropriately coupled with Cr_2O_3, an antiferromagnet that has its magnetic moments along the hexagonal *c*-axis being possible to have moments in the perpendicular direction when properly aligned[27–29]. Although Cr_2O_3 has already been coupled with ferromagnetic metals[30–32], the interaction with $Fe_{72}Ga_{28}$ seems not a trivial problem. $Fe_{72}Ga_{28}$ has already been coupled with $TbFe_2$ in [$Fe_{72}Ga_{28}$/$TbFe_2$] multilayers to turn its magnetization into the OOP direction[33,34]. However, only a tilt of the magnetization of around 25° with respect to the sample

[1]Dpto. Física de Materiales, Fac. CC. Físicas, Universidad Complutense de Madrid, Ciudad Universitaria s/n, 28040 Madrid, Spain. [2]Institute for Optoelectronic Systems and Microtechnology (ISOM), Polytechnic University of Madrid (UPM), Avenida Complutense 30, 28040 Madrid, Spain. [3]Dept Appl Phys, Univ Castilla La Mancha, Inst Reg Invest Cient Aplicada IRICA, 13071 Ciudad Real, Spain. [4]Instituto de Magnetismo Aplicado, UCM-ADIF-CSIC, 28232 Las Rozas, Spain. ✉email: rociran@ucm.es

plane was achieved despite the large PMA of $TbFe_2$[33,34]. Here we show that by means of a suitable experiment design in terms of layer thickness and materials, it is possible to reach an effective interfacial interaction that enables to turn the $Fe_{72}Ga_{28}$ magnetization into the OOP direction. In addition, because of the interfacial interaction we have observed exchange-bias effect in the perpendicular direction being possible to fit the experimental exchange-bias fields (H_E) by means of the random field model[35–37].

Experimental section

30 nm-thick Cr_2O_3 was synthetized from the evaporation of Cr on glass substrates that was subsequently oxidized in oxygen atmosphere at 750 °C during 3 h. $Fe_{72}Ga_{28}$ layers with a thickness ranging from 240 to 20 nm were grown by the DC magnetron sputtering technique in the ballistic regime at room temperature on top of the Cr_2O_3. The sputtering deposition was carried out in oblique incidence with an angle between the vapor beam and the perpendicular to the sample of about 25° and a distance of 9 cm between target and substrate. This direction of the vapor beam within the sample plane is taken as the reference direction to control the direction of the in-plane uniaxial anisotropy axis when created[16,17,38]. $Fe_{72}Ga_{28}$ films were deposited from a target with a composition of $Fe_{72}Ga_{28}$ with a diameter of 5 cm and a thickness of 2 mm using an Ar pressure of $3{\cdot}10^{-3}$ mbar and a growth power of 90 W in all cases. A 20-nm thick Mo layer was used as a capping layer to avoid FeGa oxidation. Mo was also deposited with a power of 90 W and with an Ar pressure of $3{\cdot}10^{-3}$ mbar. Therefore, the structure of the studied samples is: glass/ Cr_2O_3/$Fe_{72}Ga_{28}$/Mo. For further comparisons, we have also deposited single $Fe_{72}Ga_{28}$ layers with thickness of 20 and 150 nm between Mo buffer and capping layers to avoid oxidation.

We have used X-ray diffractometry (XRD) in the Bragg–Brentano configuration to study the structural properties. Measurements were performed in a Philips X'Pert MPD using the Cu K_α wavelength (1.54056 Å). A Digital Instruments Nanoscope IIIa instrument was used to obtain MFM images. We monitored the cantilever's phase of oscillation while the magnetic tip was scanning the sample surface to work in the phase detection mode. The distance between sample and surface was 40 nm on average (lift mode)[33]. The MFM measurements were performed without magnetic field after an OOP magnetic field of 10 kOe was applied. The topography of the samples has also been obtained in this microscope working as an Atomic Force Microscope (AFM).

In-plane and OOP hysteresis loops were performed in a vibrating sample magnetometer (VSM) from Lake-Shore 7304 at room temperature. In the sample plane, we measured loops at different angles between the applied magnetic field and the in-plane reference direction. As a reference direction, we considered as 0° the beam incidence direction in the sample plane[17,38]. Hysteresis loops at 5 K were measured in a SQUID EverCool MPMS SQUID magnetometer from Quantum Design after field-cooling (FC) at 1 kOe from 360 K and zero-field-cooling (ZFC) at 0 kOe from 360 K. To reduce any hypothetical systematic error from the SQUID, a field step of 10 Oe has been used in the low field region of the hysteresis loops. Also, the comparison between FC and ZFC hysteresis loops has been used to cross-check the shift in the field axis. At low temperature, only OOP loops were recorded. Magnetic moment versus temperature was also measured with the magnetic field in the perpendicular direction.

Results and discussion

In the XRD measurements we have only observed diffractions peaks related to either Cr_2O_3, FeGa or Mo (Fig. 1a). We have analyzed the possibility of $Fe_{72}Ga_{28}$ oxidation because of its growth on top of Cr_2O_3, but XRD measurements do not show evidences of oxidation within the resolution technique. The diffraction peaks related to FeGa are similar to what we have previously reported about sputtered $Fe_{72}Ga_{28}$ thin films being the (110) the main diffraction peak[16–19]. For $Fe_{72}Ga_{28}$ we can determine the lattice parameter (a) thanks to Bragg's law:

$$n = 2d_{hkl}sin\theta \tag{1}$$

where d_{hkl} is the family of planes,θ the diffraction angle, and λ the radiation wavelength (Cu K_α in this case). In the cubic system, we can obtain a from d_{hkl} since:

$$a = d_{hkl}\left(h^2 + k^2 + l^2\right) \tag{2}$$

where h, k, and l are the Miller indexes of the family of planes. From experimental results for the (110) peak we have determined a lattice parameter of 2.90 Å, in agreement with previous works[17,18].

On the other hand, the diffraction peaks of Cr_2O_3 show no variations upon the deposition of $Fe_{72}Ga_{28}$ on top of it as it can be inferred from the comparison with a single layer of Cr_2O_3 deposited in the same growth conditions (Fig. 1a). Experimental diffraction peaks for Cr_2O_3 appear at the same diffraction angles than for the file used for identification (01-084-0312) and therefore, it has a rhombohedral structure with lattice parameters $a = b = 4.95$ Å and $c = 13.56$ Å. Cr_2O_3 layers are not fully c-oriented since (012), (104) and (116) diffraction peaks for Cr_2O_3 have been detected by XRD. However, it is expected a magnetic contribution along the perpendicular direction due to these family of planes. The Nèel temperature (T_N) of the Cr_2O_3 has been obtained from the measurement of the magnetization as a function temperature (Fig. 1b). The experimental value of $T_N = 297$ K is just 10 K below that of bulk Cr_2O_3, $T_N = 307$ K. Finally, we have also analysed the morphology of the samples by AFM (Fig. 2) being obtained a root mean square (rms) roughness of around 2 nm for the final stack.

Sputtered $Fe_{72}Ga_{28}$ layers deposited in the ballistic regime develop in-plane magnetic anisotropy above 100 nm[16,18]. Nevertheless, the coupling with Cr_2O_3 completely eliminate this in-plane anisotropy even for thicknesses well above 100 nm (Fig. 3a). This can be understood considering that a sample will show PMA if two conditions are fulfilled: i) it is magnetically isotropic in the sample plane, and ii) the OOP direction is an easy axis in comparison to any direction in the sample plane. Therefore, the absence of in-plane magnetic anisotropy is a necessary condition for the PMA to be developed. We have ruled out that magnetostriction and strain have any effect on this modification of the magnetic anisotropy since we have not observed differences of the $Fe_{72}Ga_{28}$

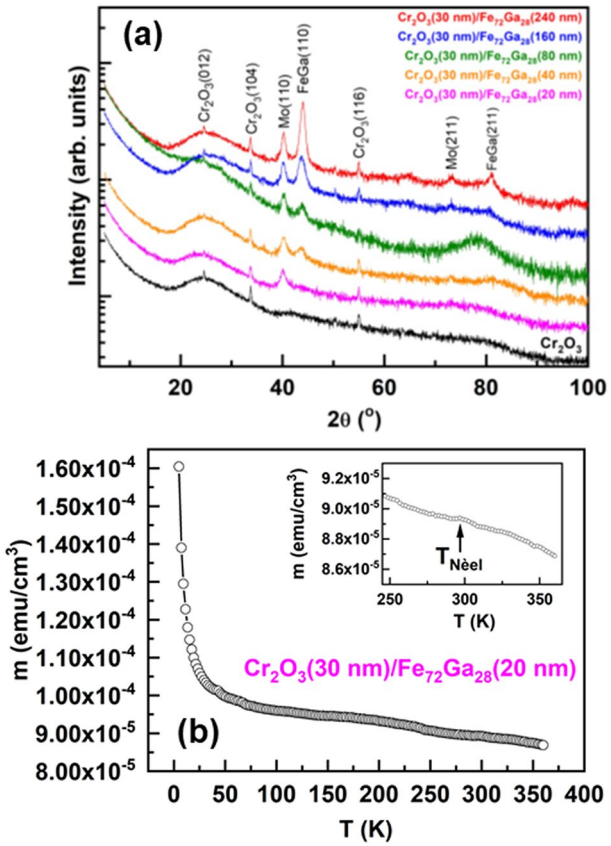

Figure 1. (**a**) XRD diffraction patterns of the samples studied in this work. The measurement for a 30 nm-thick Cr_2O_3 layer on glass has been included for further comparisons. Curves are shifted for clarity. (**b**) Magnetic moment versus temperature for the $Cr_2O_3/Fe_{72}Ga_{28}$(20 nm) sample. Inset: Detail of the measurement.

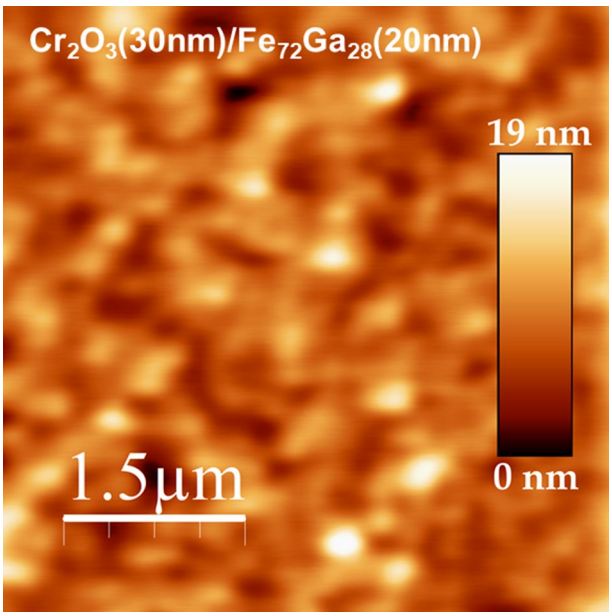

Figure 2. Morphology of the sample Cr_2O_3(30 nm)/$Fe_{72}Ga_{28}$(20 nm) measured by AFM in an area of 5 μm × 5 μm.

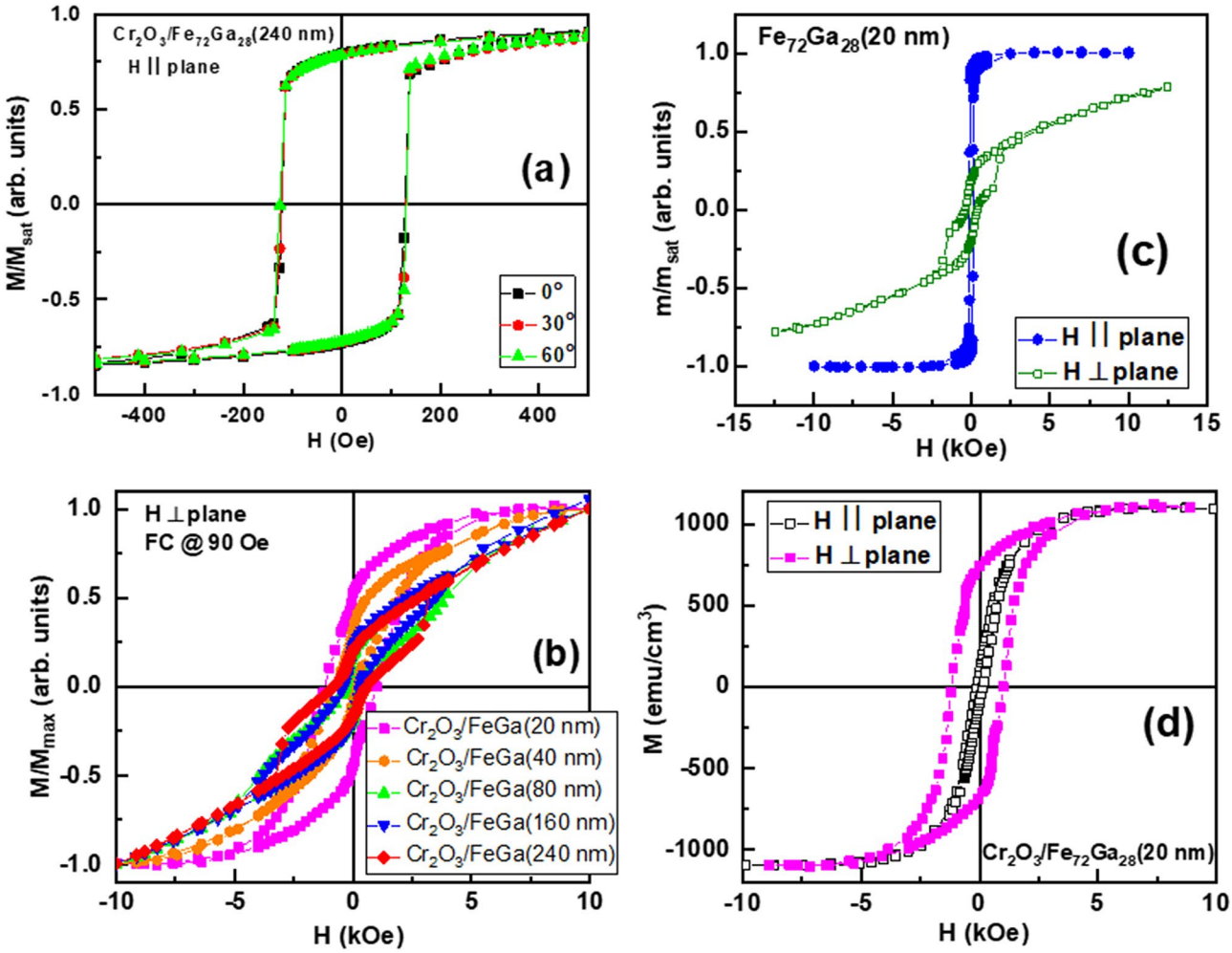

Figure 3. (**a**) In-plane room temperature hysteresis loops recorded for different angles between the reference direction taken as the reference beam direction and the applied magnetic field (filled square) 0°, (filled circle) 30°, and (filled triangle) 60° for the $Cr_2O_3/Fe_{72}Ga_{28}$(240 nm) sample. (**b**) OOP hysteresis loops recorded at room temperature for samples with different FeGa thickness (filled square) 20 nm, (filled circle) 40 nm, (filled triangle) 80 nm, (filled down triangle) 160 nm, and (filled diamond) 240 nm. (**c**) In plane and perpendicular hysteresis loops at room temperature for an uncoupled 20 nm $Fe_{72}Ga_{28}$ thin film. (**d**) Comparison of in plane (open square) and perpendicular (filled square) hysteresis loops at room temperature for the $Cr_2O_3/Fe_{72}Ga_{28}$(20 nm) sample.

	$Cr_2O_3/Fe_{72}Ga_{28}$ system FeGa thickness (nm)					Single $Fe_{72}Ga_{28}$ thickness (nm)
$Fe_{72}Ga_{28}$ thickness (nm)	20	40	80	160	240	20
M_r/M_{max} (OOP direction)	0.5	0.3	0.2	0.2	0.2	0.2
Perpendicular K_{FM} (erg/cm^3)	$2.8 \cdot 10^6$	$3.3 \cdot 10^6$	–	–	–	–

Table 1. OOP squareness (M_r/M_{max}) calculated from the perpendicular hysteresis loops as a function of the $Fe_{72}Ga_{28}$ thickness in the $Cr_2O_3/Fe_{72}Ga_{28}$ system, and for an uncoupled single $Fe_{72}Ga_{28}$ layer. Perpendicular magnetic anisotropy (K_{FM}) for the $Cr_2O_3/Fe_{72}Ga_{28}$ system in those samples in which the OOP direction is a clear easy axis.

lattice parameter with respect to uncoupled single layers. In fact, when strain has been used to manipulate the magnetic anisotropy in Ga-rich FeGa thin films, only the direction within the sample plane was modified[20].

The VSM hysteresis loops reveal the change of the magnetization direction from in-plane to OOP as the $Fe_{72}Ga_{28}$ thickness is reduced (Fig. 3b). We can quantitively monitor this evolution by means of the OOP squareness (M_r/M_{max}) defined as the ratio between the remanence (M_r) and the maximum magnetization (M_{max}) obtained in the perpendicular hysteresis loops. In Table 1 we can observe how the squareness increases as the

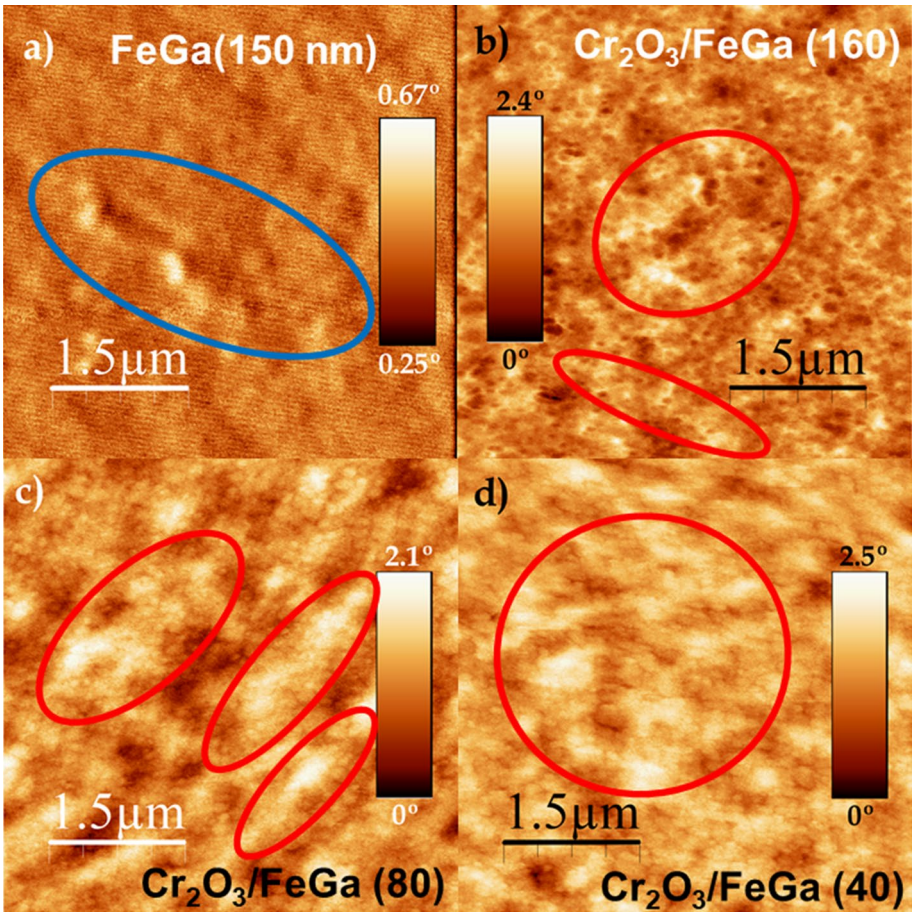

Figure 4. MFM images taken at remanence after an applied magnetic field of 10 kOe was applied in the perpendicular direction. (**a**) 150 nm-thick uncoupled $Fe_{72}Ga_{28}$ layer. With a blue line it is indicated an example of the magnetic contrast known as ripple. (**b**) $Cr_2O_3/Fe_{72}Ga_{28}$(160 nm), (**c**) $Cr_2O_3/Fe_{72}Ga_{28}$(80 nm), and (**d**) $Cr_2O_3/Fe_{72}Ga_{28}$(40 nm). In (**b**), (**c**) and (**d**), a red line is used to highlight examples of areas where magnetic stripes can be observed.

$Fe_{72}Ga_{28}$ thickness is reduced, mostly for a thickness below 80 nm. The OOP squareness and hysteresis loops of coupled layers can be compared with those of a $Fe_{72}Ga_{28}$ thin film grown in similar conditions (Table 1; Fig. 3c). The OOP squareness of a single layer is much lower with respect to that of a $Fe_{72}Ga_{28}$ with the same thickness but coupled to Cr_2O_3. Finally, in Fig. 3d it is presented the comparison between in-plane and OOP hysteresis loops for the $Cr_2O_3/Fe_{72}Ga_{28}$(20 nm) sample to show the magnetization direction has been turned into the perpendicular direction becoming the OOP direction an easy axis.

The perpendicular magnetic anisotropy, K_{FM}, can be experimentally inferred taking into account that:

$$K_{FM} = \frac{M_{FM} \cdot H_K}{2} \tag{3}$$

being M_{FM} the saturation magnetization of the $Fe_{72}Ga_{28}$, and H_K the anisotropy field in the hard direction. For the samples with $Fe_{72}Ga_{28}$ thickness of 20 nm and 40 nm the in-plane is a hard axis, and we have obtained an average value of K_{FM} of $3{\cdot}10^6$ erg cm^{-3} (Table 1) for a M_{FM} = 1100 emu cm^{-3}[26]. For higher $Fe_{72}Ga_{28}$ thickness, the OOP direction is not a clear easy axis due to the progressive turning of the magnetization into the perpendicular direction as the FeGa thickness is reduced.

MFM images can also be used to monitor the influence of the Cr_2O_3 on the $Fe_{72}Ga_{28}$ magnetic behavior (Fig. 4). When $Fe_{72}Ga_{28}$ is no coupled (Fig. 4a), it is observed the magnetic contrast known as magnetic ripple in agreement with previous works[24–26]. However, due to the interfacial coupling with Cr_2O_3, the OOP component of the magnetization of $Fe_{72}Ga_{28}$ is enhanced, and stripe domains start to be visible in the MFM images (Fig. 4b–d).

In ferromagnetic materials with PMA, the quality factor Q is defined as[39]:

$$Q = K_{FM}/2\pi M_{FM}^2 \tag{4}$$

For materials with moderate or low PMA, $Q < 1$, stripe domains appear above a critical thickness (t_{cr}):

$$t_{cr} = 2\pi \sqrt{A_{ex}/K_{FM}} \tag{5}$$

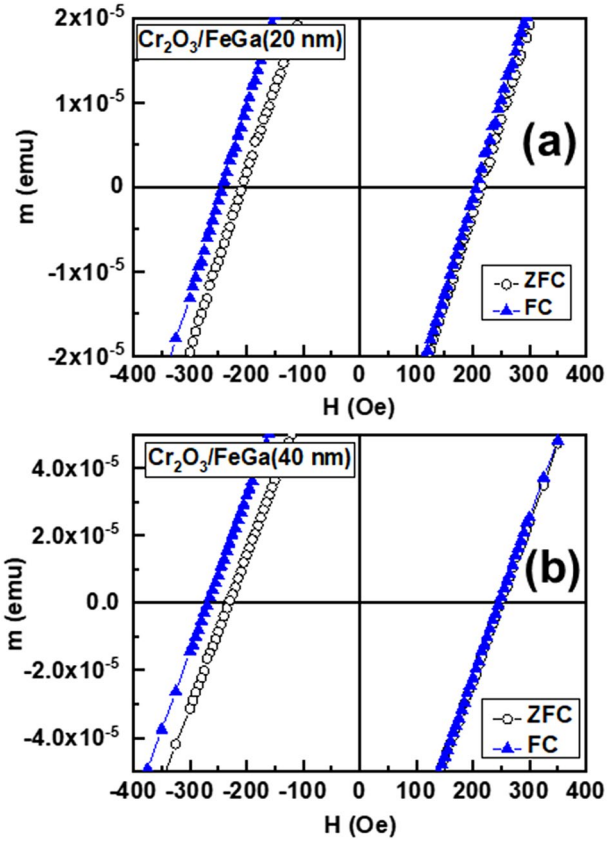

Figure 5. OOP hysteresis loops recorded at 5 K after FC at 1 kOe (filled triangle) and ZFC (open circle) from 360 K for samples with a FeGa thickness of (**a**) 20 nm, and (**b**) 40 nm.

where A_{ex} is the exchange energy per unit length. When $Q > 0.1$, stripe domains are wider than the layer thickness, whereas they exhibit a periodicity equals to the layer thickness if $Q < 0.1$.

Taking into account the experimental value inferred for the perpendicular magnetic anisotropy, $K_{FM} = 3{\cdot}10^6$ erg/cm^3, and $M_{FM} = 1100$ emu cm^{-3}[26], it is inferred a Q of 0.3 in our samples and therefore, stripes are expected above a critical thickness. Considering $A_{ex} = 1.7{\cdot}10^{-6}$ erg cm^{-1} from the literature[22,23,40], and using Eq. (5), it is obtained an experimental t_{cr} of 44 nm. This is in agreement with our experimental findings in which stripes have only been observed for $Fe_{72}Ga_{28}$ thickness ≥ 40 nm. In fact, if we take this experimental value as t_{cr}, a K_{FM} of $4{\cdot}10^6$ erg cm^{-3} is calculated, close to the experimental inferred value from experimental hysteresis loops, $3{\cdot}10^6$ erg cm^{-3}. Finally, from the MFM images we have obtained a stripe period between 110 and 125 nm by means of the power spectral density (supplementary information). This stripe periodicity higher than the layer thickness is consistent with the quality factor Q higher than 0.1 calculated in our samples.

In addition to the rotation of the $Fe_{72}Ga_{28}$ direction magnetization towards the perpendicular direction, we have observed an exchange-bias effect related to the Cr_2O_3/ $Fe_{72}Ga_{28}$ interfacial coupling as indicated by the shift of the OOP hysteresis loop in the horizontal axis (H_E) at 5 K after a FC process at 1 kOe (Fig. 5). This exchange-bias phenomenon in the perpendicular direction is related to the exchange-coupling between the antiferromagnetic Cr_2O_3, and the ferromagnetic $Fe_{72}Ga_{28}$[41]. For a $Fe_{72}Ga_{28}$ thickness of 20 nm, H_E is − 21 Oe, and − 11 Oe for a thickness of 40 nm. For the lowest FeGa thickness, exchange-bias effect has been observed at least up to 200 K.

Since the perpendicular magnetic anisotropy inferred in this work for $Fe_{72}Ga_{28}$ ($K_{FM} = 3{\cdot}10^6$ erg·cm^{-3}) is higher than the theoretical value of Cr_2O_3 ($K_{AF} = 2{\cdot}10^5$ erg·cm^{-3})[42], and some chemical roughness is expected at the $Fe_{72}Ga_{28}/Cr_2O_3$ interface, we have used the random field model proposed by Malozemoff[35–37] to calculate the theoretical H_E values. In this random field model, the AF layer breaks into domains, and the exchange-bias field is obtained by means of the expression:

$$H_E = \frac{2z\sqrt{A_{AF}K_{AF}}}{\pi^2 M_{FM} t_{FM}} \tag{6}$$

where z is generally taken as the unity, and A_{AF} is the exchange stiffness of the antiferromagnet that takes a value of $4{\cdot}10^{-7}$ erg cm^{-1}[42]. With this expression (6) we obtain H_E equals to − 26 Oe and − 13 Oe for $Fe_{72}Ga_{28}$ thickness of 20 and 40 nm, respectively, that are pretty close to the experimental − 21 Oe and − 11 Oe, respectively. This well agreement confirms the possibility of using this model in Cr_2O_3-based exchange-biased systems as also previously reported[42].

Finally, from H_E experimental values the interfacial exchange energy ΔE can be calculated:

$$\Delta E = H_E M_{FM} t_{FM} \quad (7)$$

For $Fe_{72}Ga_{28}$ of 20 nm and 40 nm, it is obtained a ΔE of 0.046 and 0.048 erg cm^{-2} that is similar than reported in previous works in which Cr_2O_3 has been coupled with other ferromagnets with values of 0.05 erg cm^{-2} at 5 K[30,41]. However, it is important to remark that we have obtained that interfacial energy using polycrystalline Cr_2O_3, not a fully *c*-oriented Cr_2O_3 with all the magnetic moments aligned in the perpendicular direction. Nevertheless, our experimental results point out that even in this situation, it is possible to gradually turn the $Fe_{72}Ga_{28}$ magnetization into the out of plane direction due to the combination of Cr_2O_3 with $Fe_{72}Ga_{28}$ that has a magnetic fluctuation that promotes magnetic ripple in the uncoupled layers[25]. Therefore, these results show the possibility of using polycrystalline layers for further applications such as tailoring of the magnetization direction.

Conclusions

In summary, we have studied the effect of the interfacial coupling between an antiferromagnet with magnetic moments along the *c*-axis (Cr_2O_3) and a ferromagnet ($Fe_{72}Ga_{28}$) with the magnetization in the sample plane but with a fluctuation that produces magnetic ripple. First of all, the in-plane magnetic anisotropy of $Fe_{72}Ga_{28}$ is completely vanished due to the coupling. Secondly, stripe domains are promoted due to the enhancement of the OOP component of the $Fe_{72}Ga_{28}$ magnetization. We have observed that the magnetization direction of $Fe_{72}Ga_{28}$ is gradually turned from in-plane to the OOP direction as the $Fe_{72}Ga_{28}$ thickness is reduced A perpendicular magnetic anisotropy of $3{\cdot}10^6$ erg·cm^{-3} has been inferred from experimental results in the $Fe_{72}Ga_{28}$ layers. It has also been observed exchange-bias phenomena in the perpendicular direction fitting the experimental data to the random field model.

Received: 6 April 2021; Accepted: 10 June 2021
Published online: 28 June 2021

References

1. S. Chikazumi. *Physics of Ferromagnetism*. Oxford Science Publications (1997).
2. Fert, A., Reyren, N. & Cros, V. Magnetic skyrmions: Advances in physics and potential applications. *Nat. Rev. Mater.* **2**, 17031 (2017).
3. Dieny, B. & Chshiev, M. Perpendicular magnetic anisotropy at transition metal/oxide interfaces and applications. *Rev. Mod. Phys.* **89**, 025008 (2017).
4. Sbiaa, R., Meng, H. & Piramanayagam, S. N. Materials with perpendicular magnetic anisotropy for magnetic random access memory. *Phys. Status Solidi RRL* **5**, 413 (2011).
5. Umadevi, K., Bysakh, S., Arout Chelvane, J., Kamat, S. V. & Jayalaskhmi, V. Tailoring magnetic anisotropy in Tb–Fe–Co thin films by rapid thermal annealing. *J. Alloys Compd.* **663**, 430 (2016).
6. Sander, D. *et al.* The 2017 magnetism roadmap. *J. Phys. D Appl. Phys.* **50**, 363001 (2017).
7. Sbiaa, R., Law, R., Tan, E.-L. & Liew, T. Spin transfer switching enhancement in perpendicular anisotropy magnetic tunnel junctions with a canted in-plane spin polarizer. *J. Appl. Phys.* **105**, 013910 (2009).
8. Krivorotov, I. N. *et al.* Time-domain measurements of nanomagnet dynamics driven by spin-transfer torques. *Science* **307**, 228 (2005).
9. Garnier, L.-C. *et al.* Stripe domains reorientation in ferromagnetic films with perpendicular magnetic anisotropy. *J. Phys. Mater.* **3**, 024001 (2020).
10. Romera, M., Ranchal, R., Ciudad, D., Maicas, M. & Aroca, C. Magnetic properties of sputtered Permalloy/molybdenum multilayers. *J. Appl. Phys.* **110**, 083910 (2011).
11. Markó, D. *et al.* Tunable ferromagnetic resonance in coupled trilayers with crossed in-plane and perpendicular magnetic anisotropies. *Appl. Phys. Lett.* **115**, 082401 (2019).
12. Coïsson, M., Barrera, G., Celegato, F. & Tiberto, P. Rotatable magnetic anisotropy in $Fe_{78}Si_9B_{13}$ thin films displaying stripe domains. *Appl. Surf. Sci.* **476**, 402 (2019).
13. Ranchal, R. & Maestre, D. Growth and characterization of $Fe_{1-x}Ga_x$ thin films from citrate-based electrolytes. *J. Phys. D Appl. Phys.* **47**, 355004 (2014).
14. Clark, A. E., Restorff, J. B., Wun-Fogle, M., Lograsso, T. A. & Schlagel, D. L. Magnetostrictive properties of body-centered cubic Fe–Ga and Fe–Ga–Al alloys. *IEEE Trans. Magn.* **36**, 3238 (2000).
15. Clark, A. E., Wun-Fogle, M., Lograsso, T. A. & Cullen, J. R. Effect of quenching on the magnetostriction on $Fe_{1-x}Ga_x$ ($0.13 < x < 0.21$). *IEEE Trans. Magn.* **37**, 2678 (2001).
16. Bartolomé, P., Begué, A., Muñoz-Noval, A., Ciria, M. & Ranchal, R. Unveiling the different physical origins of magnetic anisotropy and magnetoelasticity in Ga-Rich FeGa thin films. *J. Phys. Chem. C* **124**, 4717 (2020).
17. Muñoz-Noval, A., Ordóñez-Fontes, A. & Ranchal, R. Influence of the sputtering flow regime on the structural properties and magnetic behavior of Fe–Ga thin films (Ga ~ 30 at.%). *Phys. Rev. B* **93**, 214408 (2016).
18. Muñoz-Noval, A., Fin, S., Salas-Colera, E., Bisero, D. & Ranchal, R. The role of surface to bulk ratio on the development of magnetic anisotropy in high Ga content $Fe_{100-x}Ga_x$ thin films. *J. Alloys Compd.* **745**, 413 (2018).
19. Muñoz-Noval, A., Salas-Colera, E. & Ranchal, R. Local and medium range order influence on the magnetic behavior of sputtered Ga-rich FeGa thin films. *J. Phys. Chem. C* **123**, 13131 (2019).
20. Hontecillas, I., Figueruelo, I., Abad, S. & Ranchal, R. Tuning the magnetic anisotropy of Ga-rich FeGa thin films deposited on rigid substrates. *J. Magn. Magn. Mater.* **494**, 165771 (2020).
21. Barturen, M. *et al.* Crossover to striped magnetic domains in $Fe_{1-x}Ga_x$ magnetostrictive thin Films. *Appl. Phys. Lett.* **101**, 092404 (2012).
22. Tacchi, S. *et al.* Rotatable magnetic anisotropy in a Fe0.8Ga0.2 thin film with stripe domains: Dynamics versus statics. *Phys. Rev. B* **89**, 024411 (2014).
23. Fin, S. *et al.* In-plane rotation of magnetic stripe domains in $Fe_{1-x}Ga_x$ thin films. *Phys. Rev. B* **92**, 224411 (2015).
24. Ranchal, R., Fin, S. & Bisero, D. Magnetic microstructures in electrodeposited Fe1−xGax thin films ($15 \le x \le 22$ at.%). *J. Phys. D: Appl. Phys.* **48**, 075001 (2015).
25. Bartolomé, P., Maicas, M. & Ranchal, R. Out of plane component of the magnetization of sputtered $Fe_{72}Ga_{28}$ layers. *J. Magn. Magn. Mater.* **514**, 167183 (2020).

26. Begué, A., Proiettia, M. G., Arnaudas, J. I. & Ciria, M. Magnetic ripple domain structure in FeGa/MgO thin films. *J. Magn. Magn. Mater.* **498**, 166135 (2020).
27. Kosub, T. *et al.* Purely antiferromagnetic magnetoelectric random access memory. *Nat. Commun.* **8**, 13985 (2017).
28. Fallarino, L., Binek, C. & Berger, A. Boundary magnetization properties of epitaxial $Cr_{2-x}Al_xO_3$ thin films. *Phys. Rev. B* **91**, 214403 (2015).
29. He, X. *et al.* Robust isothermal electric control of exchange bias at room temperature. *Nat. Mater.* **9**, 579 (2010).
30. Lin, K.-W. & Guo, J.-Y. Tuning in-plane and out-of-plane exchange biases in $Ni_{80}Fe_{20}$/Cr-oxide bilayers. *J. Appl. Phys.* **104**, 123913 (2008).
31. Yuan, W. *et al.* Crystal structure manipulation of the exchange bias in an antiferromagnetic film. *Sci. Rep.* **6**, 28397 (2016).
32. Nozaki, T. *et al.* Positive exchange bias observed in Pt-inserted Cr_2O_3/Co exchange coupled bilayers. *Appl. Phys. Lett.* **105**, 212406 (2014).
33. Bartolomé, P., Maicas, M., Biskup, N., Varela, M. & Ranchal, R. Investigation of the out of plane component of the magnetization of $[Fe_{72}Ga_{28}(x\ nm)/Tb_{33}Fe_{67}(50\ nm)]_2$ multilayers. *Phys. Status Solidi A* **215**, 1800183 (2018).
34. Bartolomé, P. & Ranchal, R. Synthetic domain walls in $[TbFeGa/TbFe]_2$ multilayers. *Nanotechn.* **31**, 335715 (2020).
35. Malozemoff, A. P. Random-field model of exchange anisotropy at rough ferromagnetic-antiferromagnetic interfaces. *Phys. Rev. B* **35**, 3679 (1987).
36. Malozemoff, A. P. Mechanisms of exchange anisotropy. *J. Appl. Phys.* **63**, 3874 (1988).
37. Malozemoff, A. P. Heisenberg-to-Ising crossover in a random-field model with uniaxial anisotropy. *Phys. Rev. B* **37**, 7673 (1988).
38. Maicas, M., Ranchal, R., Aroca, C., Sánchez, P. & López, E. Magnetic properties of permalloy multilayers with alternating perpendicular anisotropies. *Eur. Phys. J. B* **62**, 267 (2008).
39. Hubert, A. & Schäfer, R. *Magnetic Domains: The Analysis of Magnetic Microstructures*. Springer (2008).
40. Gopman, D. B., Sampath, V., Ahmad, H., Bandyopadhyay, S. & Atulasimha, J. Static and dynamic magnetic properties of sputtered Fe–Ga thin films. *IEEE Trans. Magn.* **53**, 6101304 (2017).
41. Nogués, J. & Schuller, I. K. Exchange bias. *J. Magn. Magn. Mater.* **192**, 203 (1999).
42. Zheng, R. K., Liu, H., Wang, Y. & Zhang, X. X. Cr_2O_3 surface layer and exchange bias in an acicular CrO_2 particle. *Appl. Phys. Lett.* **84**, 702 (2004).

Acknowledgements

"CAI Difracción Rayos-X" from UCM is acknowledged for XRD measurements. This work has been financially supported through the projects RTI2018-097895-B-C43 of the Spanish Ministry of Science, Innovation, and Universities, MAT2017-87072-C4-3-P of the Spanish Ministry of Economy, Industry and Competitiveness, and 'Plan Propio de la Universidad de Castilla – La Mancha' (FEDER, EU) for the 'Grupo de Materiales Magnéticos (GMM)'. The data that support the findings of this study are available from the corresponding author upon reasonable request.

Author contributions

I.H. grew part of the samples and magnetically characterized the samples by VSM and MFM. M.M performed part of the MFM experiments, and helped with VSM measurements. J.P.A. helped with the VSM and performed SQUID experiments. RR. thought the experiments, and grew part of the samples. All authors contributed to the discussion of the results. R.R wrote the main manuscript. All authors reviewed the manuscript.

Competing interests

The authors declare no competing interests.

Additional information

Supplementary Information The online version contains supplementary material available at https://doi.org/10.1038/s41598-021-92640-y.

Correspondence and requests for materials should be addressed to R.R.

Reprints and permissions information is available at www.nature.com/reprints.

Publisher's note Springer Nature remains neutral with regard to jurisdictional claims in published maps and institutional affiliations.